



HAL
open science

Optimal control problem in treatment strategies for breast tumors

Enagnon David Lassounon, Aziz Belmiloudi, Mounir Haddou

► **To cite this version:**

Enagnon David Lassounon, Aziz Belmiloudi, Mounir Haddou. Optimal control problem in treatment strategies for breast tumors. 2024. hal-04681556v1

HAL Id: hal-04681556

<https://hal.science/hal-04681556v1>

Preprint submitted on 29 Aug 2024 (v1), last revised 12 Nov 2024 (v2)

HAL is a multi-disciplinary open access archive for the deposit and dissemination of scientific research documents, whether they are published or not. The documents may come from teaching and research institutions in France or abroad, or from public or private research centers.

L'archive ouverte pluridisciplinaire **HAL**, est destinée au dépôt et à la diffusion de documents scientifiques de niveau recherche, publiés ou non, émanant des établissements d'enseignement et de recherche français ou étrangers, des laboratoires publics ou privés.

Optimal control problem in treatment strategies for breast tumors

David Lassounon¹, Aziz Belmiloudi², and Mounir Haddou³

¹ Univ Rennes, INSA, CNRS, IRMAR-UMR 6625, F-35000 Rennes, France
`enagnon-david.lassounon@insa-rennes.fr`

² Univ Rennes, INSA, CNRS, IRMAR-UMR 6625, F-35000 Rennes, France
`aziz.belmiloudi@insa-rennes.fr`

³ Univ Rennes, INSA, CNRS, IRMAR-UMR 6625, F-35000 Rennes, France
`mounir.haddou@insa-rennes.fr`

Abstract. In this work, we present an optimal control problem under state constraints for breast cancer treatment by chemotherapy. In this instance, the drug dosage is considered as a control variable. Since chemotherapeutic agents affect both tumor cells and healthy cells, the main goal of the control problem is to minimize the evolution of tumor cells with less possible damage to the normal tissue. A system of nonlinear reaction-diffusion equations is used to describe the drug concentration in the tumor cells. The optimal control problem is formulated by specifying a performance criterion and different kinds of constraints, and the necessary optimality conditions are investigated. Afterward, numerical simulations with realistic data are presented and discussed to demonstrate the importance of suggesting optimal control strategies for tumor cell dynamics and eradication. Finally, the conclusion and the future perspectives are presented.

Keywords: Optimal control theory · state constraints · cancer chemotherapy · nonlinear reaction-diffusion systems · malignant tumors · numerical simulations.

1 Introduction and Motivation

One of the leading causes of death among women worldwide is breast cancer. It's a disease characterized by the uncontrolled growth of abnormal breast cells, which then form malignant tumors. The earliest form is not life-threatening and can be detected early. Malignant tumor cells spread to nearby breast tissue through invasion. Invasive cancers then spread to the lymph nodes in the breast, forming metastases that allow them to migrate to other organs such as the lungs, brain, and liver. Among the different therapies for breast cancer, chemotherapy is the most widely used treatment for the eradication of most cancers [6], using cytotoxic drugs that promote cell death and are administered systemically in the whole body. Difficulties in modeling chemotherapies lie in the acute toxicity of drugs on normal breast cells and the resistance of tumors to drugs. Several mathematical models have proposed to describe the effect of chemotherapy on tumor

growth [3, 7–9], and very recently, other mathematical models called treatment response models directly using data from quantitative medical imaging have been formulated [1, 2, 10]. The importance of treatment response models lies in the fact that they integrate clinical or experimental data to predict the response of tumors to treatments and allow testing of the effectiveness of different therapies. In [2], an optimal chemotherapy strategy was studied. It was found that when control constraints were imposed, tumor cell density was less responsive to treatment. It would, therefore, be interesting to have, in addition to constraints on the drug, a dynamic constraint on the density of tumor cells, forcing it to respond to treatment. This which helps to treat malignant cancers. To study the evolution of tumor density in the breast subjected to chemotherapy, we consider the following nonlinear parabolic equation described by

$$\begin{cases} \frac{\partial \vartheta}{\partial t} = \operatorname{div}(\kappa \nabla \vartheta) - \Psi_1 \vartheta^3 + \Psi_2 \vartheta - \alpha_0 \phi \vartheta & \text{in } \mathcal{Q}, \\ -\kappa \nabla \vartheta \cdot \mathbf{n} = \Psi_3 \vartheta^2 & \text{on } \Sigma, \\ \vartheta(t = 0, \mathbf{x}) = \vartheta_0(\mathbf{x}) & \text{in } \Omega, \end{cases} \quad (1)$$

under the constraint

$$\varphi_0(\mathbf{x}) \leq \phi(t, \mathbf{x}) \leq \varphi_1(\mathbf{x}) \quad a.e. (\mathbf{x}, t) \in \mathcal{Q}, \quad (2)$$

and the state constraint

$$G(\phi) = \|\vartheta(t, \cdot)\|_{L^2(\Omega)}^2 - \xi_\vartheta(t) \leq 0 \quad a.e. t \in (0, T). \quad (3)$$

The breast domain Ω is an open bounded domain in \mathbb{R}^2 with a smooth boundary $\Gamma = \partial\Omega$, $T > 0$ is a given final time, $\mathcal{Q} = (0, T) \times \Omega$, $\Sigma = (0, T) \times \Gamma$ and the vector \mathbf{n} is the outward normal to Γ . The value $\vartheta(t, \mathbf{x})$ is the tumoral density at time t and position \mathbf{x} in Ω and the function Ψ_1 is the intrinsic growth rate. The function Ψ_2 is the tumor proliferation rate, and Ψ_3 is the migration capacity of tumor cells to other organs. The quantity $\phi \vartheta$ is the treatment term describing the death of cells due to chemotherapy treatment, in which the control value $\phi(t, \mathbf{x})$ models the concentration of drugs in chemotherapy treatment at time t and position \mathbf{x} and ϑ_0 is the density of tumor at time initial time $t = 0$. The diffusivity function of the tumor cells is defined in \mathcal{Q} and satisfies $0 < \varsigma_0 \leq \kappa(t, \mathbf{x}) \leq \varsigma_1$, where ς_0 and ς_1 are two positives constants. The functions ξ , φ_0 and φ_1 are sufficiently regular. It is worth noting that the nonlinear system (1) integrates a control ϕ dependent on time and position and considers the capacity of invasion and migration of cancer cells to other organs modeled by the function Ψ_3 . This consideration is neglected (see, e.g., [1–3, 10, 11]). Note that, for an intracranial brain tumor such as glioblastoma or astrocytoma, the migration capacity $\Psi_3 = 0$, because the cranial vault does not allow volume expansion of tumor cells but in the breast or lung, $\Psi_3 \neq 0$, since we can witness a significant flow of tumor cells migrating to other organs by spreading to the lymph nodes of the breast. Moreover, the control limit functions φ_0, φ_1 are medical and patient-specific.

The inequality constraint (2) imposed on the control ϕ makes it possible to avoid acute toxicity of chemotherapeutic drugs beyond the drug concentration limit.

2 Assumptions and Notations

In this section, we introduce the following spaces and some notations.

For $p \in]1; +\infty[$ and $s \in [0; 1/2[$ we denote by

$$\begin{aligned} L_+^p(\mathcal{Q}) &= \{u \in L^p(\mathcal{Q}); \quad u \geq 0\}, \quad \mathcal{Z}_s = H^{2s+1}(\Omega), \\ \mathcal{X}_s &= L^2(0, T; \mathcal{Z}_s), \quad \mathcal{W}_s = H^1(0, T; \mathcal{Z}'_s), \quad \mathcal{U}_s = \mathcal{X}_s \cap \mathcal{W}_s \cap C([0, T]; \mathcal{Z}_0) \end{aligned}$$

where \mathcal{Z}'_s is the topological dual of \mathcal{Z}_s . We note u_+ the positive part of u by $u_+ = \max(u, 0)$. We can now give the weak formulation of the system (1). (for all $v \in \mathcal{Z}_0$, and *a.e* $t \in (0; T)$, $\vartheta(t = 0, \mathbf{x}) = \vartheta_0(\mathbf{x})$ in Ω):

$$\int_{\Omega} \left(\frac{\partial \vartheta}{\partial t} v + \kappa \nabla \vartheta \cdot \nabla v + \Psi_1 \vartheta^3 v - \Psi_2 \vartheta v + \alpha_0 \phi v \right) d\mathbf{x} + \int_{\Gamma} \Psi_3 \vartheta^2 v d\mathbf{x} = 0. \quad (4)$$

We state the following hypothesis that the functions Ψ_i and φ_j must satisfy, for $i = 1, \dots, 3, j = 0, 1$.

(H) $\Psi_i \in L_+^\infty(\mathcal{Q})$ for $i = 1, 2$, $\Psi_3 \in L_+^\infty(\Sigma)$, and $\varphi_i \in L_+^3(\Omega)$ for $i = 0, 1$. For the initial condition ϑ_0 of system (1), we impose $\vartheta_0 \in H^1(\Omega) \cap L_+^\infty(\Omega)$, and we assume that the parameter ξ_ϑ is chosen such that

$$\xi_\vartheta = \|\vartheta_0\|_{L^2(\Omega)}^2. \quad (5)$$

According to **(H)** and [4], the system (4) admits one and unique solution ϑ in $\mathcal{U}_s \cap L_+^\infty(\mathcal{Q})$.

We end this section by giving the units of biological data for the system (1) as follows:

- The diffusion function of tumor cells $\kappa(mm^2 \cdot d^{-1})$
- The drug concentration in chemotherapy treatment $\phi(\mu\text{M})$
- The intrinsic growth rate function of tumor cells $\Psi_1(d^{-1})$
- The cell's tumor proliferation rate $\Psi_2(d^{-1})$
- The migration capacity function of tumor cells $\Psi_3(mm \cdot d^{-1})$
- The efficacy parameter of treatment $\alpha_0(\mu\text{M}^{-1} \cdot d^{-1})$
- The final time of treatment $T(d)$.

A micromolar (μM) is the number of moles per unit volume and is the usual unit of molar concentration, mm is the unit of length, and d is the days.

Contribution. Our main goal is to eradicate malignant tumor growth in the breast with as little damage as possible to normal cells. So, we impose a constraint on control to limit the acute toxicity of drugs and a dynamic constraint on

tumor density throughout treatment. We propose an optimal control approach and a numerical technique. We obtained very promising results.

Outline of the paper. The goal of this paper is to reduce the progression of malignant breast tumors with minimal damage to normal cells. We, therefore, impose a control constraint to limit the acute toxicity of drugs and a dynamic constraint on the density of tumor cells. Our numerical simulations on two examples of eradication of malignant breast tumors with realistic data gave promising results.

3 Optimal control problem

Let $\mathcal{Y}_{ad} = \{\phi \in L^3(\mathcal{Q}) : \varphi_0(\mathbf{x}) \leq \phi(t, \mathbf{x}) \leq \varphi_1(\mathbf{x}), a.e., t \in [0, T]\}$ and $\mathcal{S} : \phi \in \mathcal{Y}_{ad} \mapsto \mathcal{S}(\phi) \in \mathcal{U}_g \cap L^{\infty}_+(\mathcal{Q})$ such that $\vartheta = \mathcal{S}(\phi)$ is the unique solution of (1), corresponding to ϕ . We introduce the following cost functional \mathcal{J} , by

$$\mathcal{J}(\phi) = \frac{1}{2} \int_{\mathcal{Q}} \vartheta^2 dxdt + \frac{\varrho}{3} \int_{\mathcal{Q}} |\phi|^3 dxdt, \quad (6)$$

where the parameter $\varrho > 0$ is the price we pay for control. The optimal control problem consists of obtaining a minimizer of functional \mathcal{J} with respect to ϕ .

We will study the following problem : Find $\phi_* \in \mathcal{Y}_{ad}$ such that functional \mathcal{J} is minimized with respect to ϕ subject to problem (1) and constraints (2) and (3).

Our control problem is then

$$(\mathbf{CP}) \begin{cases} \inf_{\phi \in \mathcal{Y}_{ad}} \mathcal{J}(\phi); \\ s.t., \quad G(\phi) \leq 0. \end{cases} \quad (7)$$

The existence of optimal solutions of (CP) is proved in [4], as well as a differentiability result of \mathcal{S} . The necessary conditions of first-order optimality under certain conditions are also given in [4].

4 Numerical techniques

A new reformulation of the optimal control problem: This section presents the strategies for resolution of the control problem (CP). To take into account the different constraints, we modify the cost function \mathcal{J} by penalizing the constraints to force them to be satisfied, which leads to the modified cost function

$$\mathcal{J}_m(\phi) = \mathcal{J}(\phi) + \frac{\varrho_1}{3} \int_{\mathcal{Q}} (\varphi_0 - \phi)_+^3 dxdt + \frac{\varrho_2}{3} \int_{\mathcal{Q}} (\phi - \varphi_1)_+^3 dxdt + \frac{\varrho_3}{4} \int_0^T G(\phi)_+^2 dt. \quad (8)$$

Then we solve a modified optimal control problem without constraint given by

$$(\mathbf{MCP}) \begin{cases} \inf_{\phi \in L^3(\mathcal{Q})} \mathcal{J}_m(\phi); \\ \text{subject to problem (1)}. \end{cases} \quad (9)$$

Optimality conditions: As the problem (MCP) is non-convex and without constraints, we therefore describe the necessary conditions of first-order optimality. According to [4], we know that the map \mathcal{S} is continuously differentiable and the derivative $\mathcal{S}'(\phi) : \mathbf{h} \mapsto w$ is solution of the linear parabolic problem:

$$\begin{cases} \frac{\partial w}{\partial t} - \operatorname{div}(\kappa \nabla w) + (3\Psi_1 \vartheta^2 + \alpha_0 \phi - \Psi_2)w = -\alpha_0 \mathbf{h} \vartheta \text{ in } \mathcal{Q}, \\ -\kappa \nabla w \cdot \mathbf{n} - 2\Psi_3 \vartheta w = 0 \text{ on } \Sigma, \\ w(t=0, \cdot) = 0 \text{ in } \Omega, \end{cases} \quad (10)$$

with $\vartheta = \mathcal{S}(\phi)$.

In order to derive the optimality conditions, we introduce the following adjoint problem corresponding to the primal solution ϑ .

$$\begin{cases} -\frac{\partial \tilde{\vartheta}}{\partial t} - \operatorname{div}(\kappa \nabla \tilde{\vartheta}) + (3\Psi_1 \vartheta^2 + \alpha_0 \phi - \Psi_2)\tilde{\vartheta} = \vartheta + \varrho_3 \vartheta G(\phi)_+ \text{ in } \mathcal{Q}, \\ -\kappa \nabla \tilde{\vartheta} \cdot \mathbf{n} - 2\Psi_3 \vartheta \tilde{\vartheta} = 0 \text{ on } \Sigma, \\ \tilde{\vartheta}(t=T, \cdot) = 0 \text{ in } \Omega. \end{cases} \quad (11)$$

In the sequel, we denote by $\tilde{\mathcal{S}}(\phi) = \tilde{\vartheta}$ the solution of adjoint problem corresponding to ϕ . The weak formulation of (11) is given by, for all $v \in \mathcal{Z}_0$, ($\tilde{\vartheta}(t=T, \cdot) = 0$ in Ω)

$$\begin{cases} -\int_{\Omega} \frac{\partial \tilde{\vartheta}}{\partial t} v d\mathbf{x} + \int_{\Omega} \kappa \nabla \tilde{\vartheta} \cdot \nabla v d\mathbf{x} + 2 \int_{\Gamma} \Psi_3 \vartheta \tilde{\vartheta} v d\mathbf{x} + 3 \int_{\Omega} \Psi_1 \vartheta^2 \tilde{\vartheta} v d\mathbf{x} \\ + \alpha_0 \int_{\Omega} \phi \tilde{\vartheta} v d\mathbf{x} - \int_{\Omega} \Psi_2 \tilde{\vartheta} v d\mathbf{x} = \int_{\Omega} \vartheta v d\mathbf{x} + \varrho_3 \int_{\Omega} \vartheta G(\phi)_+ v d\mathbf{x}. \end{cases} \quad (12)$$

Now, we can compute the derivative of \mathcal{J}_m defined by (8). Since all the terms are smooth including the function $G(\cdot)_+^2$ (G is continuously differentiable, and we have, $\forall \mathbf{h} \in L^3(\mathcal{Q})$, $G'(\phi) \cdot \mathbf{h} = 2 \int_{\Omega} \vartheta w d\mathbf{x}$). So, we have ($\forall \mathbf{h} \in L^3(\mathcal{Q})$):

$$\begin{aligned} \mathcal{J}'_m(\phi) \cdot \mathbf{h} &= \int_{\mathcal{Q}} (\vartheta + \varrho_3 \vartheta G(\phi)_+) w d\mathbf{x} dt \\ &\quad + \int_{\mathcal{Q}} (\varrho \phi^2 - \varrho_1 (\varphi_0 - \phi)_+^2 + \varrho_2 (\phi - \varphi_1)_+^2) \cdot \mathbf{h} d\mathbf{x} dt. \end{aligned} \quad (13)$$

Taking now $v = w$ in (12), we deduce, according to (10), that

$$\int_{\mathcal{Q}} (\vartheta + \varrho_3 \vartheta G(\phi)_+) w d\mathbf{x} dt = -\alpha_0 \int_{\mathcal{Q}} \mathbf{h} \vartheta d\mathbf{x} dt$$

and then $(\forall h \in L^3(\mathcal{Q}))$

$$\mathcal{J}'_m(\phi) \cdot h = \int_{\mathcal{Q}} (-\alpha_0 \vartheta \tilde{\vartheta} + \varrho \phi^2 - \varrho_1 (\varphi_0 - \phi)_+^2 + \varrho_2 (\phi - \varphi_1)_+^2) \cdot h \, d\mathbf{x} dt. \quad (14)$$

Consequently, the gradient of \mathcal{J}_m relative to ϕ can be given as

$$\nabla \mathcal{J}_m(\phi) = -\alpha_0 \vartheta \tilde{\vartheta} + \varrho \phi^2 - \varrho_1 (\varphi_0 - \phi)_+^2 + \varrho_2 (\phi - \varphi_1)_+^2. \quad (15)$$

Let ϕ_* be a solution of **(MCP)** and $\vartheta_* = \mathcal{S}(\phi_*)$ the associated optimal state. Since there is no constraint in (9), we have then $\nabla \mathcal{J}_m(\phi_*) = 0$, so that

$$\varrho \phi_*^2 - \alpha_0 \vartheta_* \tilde{\vartheta}_* - \varrho_1 (\varphi_0 - \phi_*)_+^2 + \varrho_2 (\phi_* - \varphi_1)_+^2 = 0, \quad (16)$$

where $\tilde{\vartheta}_* = \tilde{\mathcal{S}}(\phi_*)$ is the adjoint state corresponding to ϕ_* .

Brief description of the discrete problem: In this section, we give a numerical algorithm for solving the modified control problem **(MCP)**, using the adjoint variable. We will not provide a complete development of numerical resolution, but we will only be interested in discretizing the control problem and its resolution process. We used the algorithm **BFGS** to solve the derived nonlinear optimization problem. Then, we propose a finite element method coupled with the implicit Euler scheme for solving the continuous optimization problem. To describe the time-position discretization scheme, we introduce the finite-dimensional subspace $\mathcal{Z}_{0,h}$ of \mathcal{Z}_0 associated with \mathcal{T}_h , where $(\mathcal{T}_h)_h$ be a regular family of meshes of $\bar{\Omega}$. The subscript h stands for the meshsize. For the time discretization, we partition the interval $(0, T)$ by using the following points, $t_n = n\tau$, for $n = 0, \dots, N$ with $\tau = T/N$. For a continuous mapping $\vartheta : (0, T) \rightarrow L^2(\Omega)$, we denote the approximation of $\vartheta(t_n, \cdot)$ by ϑ_h^n , for $n = 0, \dots, N$. For a given sequence $(\vartheta_h^n)_{n=0, \dots, N}$ in $L^2(\Omega)$, we define its difference quotient as $\partial_\tau \vartheta_h^n = \frac{\vartheta_h^n - \vartheta_h^{n-1}}{\tau}$. The step is chosen sufficiently small to guarantee both the time accuracy and convergence of the solution. With the above notation, we formulate the finite approximation of the problems (9) and (1) as follows:

$$\left\{ \begin{array}{l} \text{Find } \phi_{*,h} \text{ in } \mathcal{Y}_{ad,h} \text{ wich minimize the functional} \\ \mathcal{J}_{m,h}(\phi_h) = \frac{\tau}{2} \sum_{n=1}^N \int_{\Omega} (\vartheta_h^n)^2 d\mathbf{x} + \frac{\tau}{3} \sum_{n=1}^N \int_{\Omega} |\phi_h^n|^3 d\mathbf{x} + \frac{\tau \varrho_3}{4} \sum_{n=1}^N G(\phi_h^n)_+^2 \\ \quad + \frac{\tau \varrho_2}{3} \sum_{n=1}^N \int_{\Omega} (\phi_h^n - \varphi_1)_+^3 d\mathbf{x} + \frac{\tau \varrho_1}{3} \sum_{n=1}^N \int_{\Omega} (\varphi_0 - \phi_h^n)_+^3 d\mathbf{x}, \end{array} \right. \quad (17)$$

where according to (4), $\vartheta_h^n \in \mathcal{Z}_{0,h}$ satisfying, for all $v_h \in \mathcal{Z}_{0,h}$, ($\vartheta_h^0 = \vartheta_0$ in Ω and $n = 1, 2, \dots, N$)

$$\left\{ \begin{array}{l} \int_{\Omega} \left(\partial_\tau \vartheta_h^n v_h + \kappa^n \nabla \vartheta_h^n \cdot \nabla v_h + \Psi_1^n (\vartheta_h^n)^3 v_h - \Psi_2^n \vartheta_h^n v_h \right. \\ \quad \left. + \alpha_0 \int_{\Omega} \phi_h^n \vartheta_h^n v_h \right) d\mathbf{x} + \int_{\Gamma} \Psi_3^n (\vartheta_h^n)^2 v_h d\mathbf{x} = 0. \end{array} \right. \quad (18)$$

Remark 1. We note that, the problem (18) can be written as:

$$\mathcal{F}_h(t_n, \vartheta_h^n, \frac{\vartheta_h^n - \vartheta_h^{n-1}}{\tau}) = 0,$$

where \mathcal{F}_h is a nonlinear operator. The resulting equation is solved using Newton's method under the software **FreeFem++**.

To solve the discretized finite element minimization of $\mathcal{J}_{m,h}(\phi_h^n)$ over $\mathcal{Y}_{ad,h}$, we need to calculate the gradient of $\mathcal{J}_{m,h}(\phi_h^n)$. According to (15), we can deduce

$$\nabla \mathcal{J}_{m,h}(\phi_h^n) = \varrho(\phi_h^n)^2 - \alpha_0 \tilde{\vartheta}_{\varrho_3,h}^n \vartheta_h^n - \varrho_1(\varphi_0 - \phi_h^n)_+^2 + \varrho_2(\phi_h^n - \varphi_1)_+^2, \quad (19)$$

where $\tilde{\vartheta}_{\varrho_3,h}^n = \tilde{\mathcal{S}}_{m,h}(\phi_h)$ is the solution of the following discrete adjoint problem (we use (12) and the discrete backward Euler approximation of time) (with $\tilde{\vartheta}_{\varrho_3,h}^{n+1}(T, \cdot) = 0$ for $n = 0, 1, \dots, N-1$.)

$$\left\{ \begin{array}{l} - \int_{\Omega} \partial_{\tau} \tilde{\vartheta}_{\varrho_3,h}^{n+1} \cdot v_h d\mathbf{x} + \int_{\Omega} \kappa^n \nabla \tilde{\vartheta}_{\varrho_3,h}^n \cdot \nabla v_h d\mathbf{x} + 2 \int_{\Gamma} \Psi_3^n \vartheta_h^n \tilde{\vartheta}_{\varrho_3,h}^n \cdot v_h d\mathbf{x} \\ + 3 \int_{\Omega} \Psi_1^n (\vartheta_h^n)^2 \tilde{\vartheta}_{\varrho_3,h}^n \cdot v_h d\mathbf{x} - \int_{\Omega} \Psi_2^n \tilde{\vartheta}_{\varrho_3,h}^n \cdot v_h d\mathbf{x} + \alpha_0 \int_{\Omega} \phi_h^n \tilde{\vartheta}_{\varrho_3,h}^n \cdot v_h d\mathbf{x} \\ = \int_{\Omega} \vartheta_h^n \cdot v_h d\mathbf{x} + \varrho_3 \int_{\Omega} \vartheta_h^n G(\vartheta_h^n)_+ \cdot v_h d\mathbf{x} \end{array} \right. \quad (20)$$

Now we give the optimization algorithm for the resolution of control problem.

Optimization algorithm: According to the previous discrete formula (19) and (20), we can now present the following **BFGS** scheme to solve the discrete minimization problem (17) and (18). For $k = 1, \dots$ (the iteration index), we denote by $\phi_{h,k}$ the numerical approximation of the control at the k^{th} iteration of the algorithm.

1. Initialisation: $\phi_{h,0}$ (given).
2. Compute the discrete primal problem (18) with the control $\phi_{h,k}$, gives $\vartheta_{h,k}^n$; for $n = 1, 2, \dots, N$.
3. Compute the discrete adjoint problem (20) (based on $(\phi_{h,k}, \vartheta_{h,k}, \varrho_3)$), gives $\tilde{\vartheta}_{h,k,\varrho_3}^n$, for $n = N-1, N-2, \dots, 0$.
4. Compute the gradient of $\mathcal{J}_{m,h}$ gives

$$d_{h,k} = \varrho(\phi_{h,k})^2 - \alpha_0 \tilde{\vartheta}_{h,k,\varrho_3}^n \vartheta_{h,k} - \varrho_1(\varphi_0 - \phi_{h,k})_+^2 + \varrho_2(\phi_{h,k} - \varphi_1)_+^2.$$

5. Find $\alpha_{h,k} > 0$ such that $\mathcal{J}_{m,h}(\phi_{h,k} - \alpha d_{h,k})$ is minimized over all $\alpha > 0$.
6. Compute $\phi_{h,k+1}$:

$$\left\{ \begin{array}{l} \phi_{h,k+1} = \phi_{h,k} + s_{h,k}, \\ s_{h,k} = \alpha_{h,k} p_{h,k}, \\ B_{h,k} p_{h,k} = -d_{h,k}, \text{ with } B_{h,0} = I \text{ (the identity matrix)}, \\ r_{h,k} = d_{h,k+1} - d_{h,k}, \\ B_{h,k+1} = B_{h,k} + (r_{h,k} r_{h,k}^T) / (r_{h,k}^T s_{h,k}) - (B_{h,k} s_{h,k} s_{h,k}^T B_{h,k}) / (s_{h,k}^T B_{h,k} s_{h,k}). \end{array} \right.$$

7. If the gradient is sufficiently small (convergence) STOP end; ELSE set $k := k + 1$ and go to item 2. The discrete approximation of the optimal solution (ϕ_*, ϑ_*) is $(\phi_{h,k}, \vartheta_{h,k})$.

Remark 2. We note that the first step of the algorithm is equivalent to gradient descent, and the following steps are steadily more refined by B_k the approximation to the Hessian matrix at ϕ_k which is updated iteratively at each step.

5 Numerical simulations

In this section, we present the results of several numerical experiments for the eradication of two examples of infiltrating lobular carcinomas (malignant breast tumors that spread rapidly to other breast tissues). Precisely, we are looking for an optimal control ϕ_* (optimal concentration of chemotherapeutic drugs) whose optimal state ϑ_* (optimal density of tumor cells) decreases rapidly and satisfies the constraint (3). To calibrate the system (18), we used some realistic data from [2, 10, 11] (for $(\mathbf{x}, t) \in \bar{\Omega} \times (0, T)$)

$$\begin{aligned} \kappa &= \kappa_0 e^{-\lambda_0 \sigma}; & \sigma &= \sigma_0 e^{-\delta_0 |\mathbf{x}|^2 t}; & \Psi_1 &= \frac{k_1 - k_2 e^{-\gamma_0 \sigma}}{e^{-\gamma_0 \sigma} (1 - e^{-2\gamma_0 \sigma})}; & \Psi_2 &= \theta^2 \Psi_1; \\ \varphi_0(\mathbf{x}) &= 0; & \varphi_1(\mathbf{x}) &= \gamma_0 e^{-\gamma_1 [(x-x_1)^2 + (y-y_1)^2]}; & \Psi_3 &= k_3 \Psi_1; & \kappa_0 &= d_0 \eta_1; \\ \eta_1 &= 1 + \varsigma_1 \cos(\varsigma_2 \eta_2); & \eta_2 &= \varsigma_3 \arctan \left(\frac{y - y_0}{\varsigma_4 + \sqrt{(x - x_0)^2 + (y - y_0)^2}} \right) \end{aligned}$$

Table 1 presents the parameters that we considered in all our experiments.

Table 1. Data table

Parameters	Values and Definitions
d_0	$1.5 \text{ mm}^2 \cdot d^{-1}$: Diffusion coefficient [11]
σ_0	18 kPa: Mechanical coupling coefficient [11]
λ_0	$2.10^{-3} \text{ kPa}^{-1}$: [2, 10]
k_2	2.0 d^{-1} : Tumor cell proliferation rate [11]
k_1	4.0 d^{-1} : Coupling constant
k_3	3.0 mm : Coupling constant
δ_0	$5.55 \cdot 10^{-5} \text{ mm}^{-2} \cdot d^{-1}$: Coupling constant
α_0	$1/d \cdot \mu\text{M}$: Coupling constant [10, 2]
T	20 days: The final horizon [2, 10]
γ_0	$100 \mu\text{M}$: Coupling constant
γ_1	20 mm^2 : Coupling constant
θ	2.236 : Coupling constant (dimensionless)
ς_1	0.75 : Coupling constant
ς_2	50 : Coupling constant
ς_3	2 : Coupling constant
ς_4	10^{-4} : Coupling constant

We can now consider the following two applications of the eradication of malignant breast tumors.

5.1 Applications

(i) Case of the presence of a single tumor.

Here, we consider $\vartheta_0(\mathbf{x}) = \eta_1 e^{-\frac{1}{\varepsilon}[(x-x_0)^2+(y-y_0)^2]}$ in Ω , representing the density of tumor cells centered in (x_0, y_0) , see Fig. 1. The discretization and mesh informations are contained in Table 2.

Table 2. Discretization informations

Parameters	Value	Definitions
Δt	0.2 days (d)	Time Step
\mathbf{x}	$(x; y)$	2D space position
Δx	1 mm	Space Discretizations (x)
Δy	1 mm	Space Discretizations (y)
n_e	3184	Total Mesh Elements
n_p	1653	Total Mesh Points
$(x_0; y_0)$	$(10/3; 10/3)$	Tumor center
$(x_1; y_1)$	$(2.9; 10/3)$	
ε	0.02	

The Fig. 2 presents the time-evolution of tumor density without treatment, i.e., $\phi = 0$ in the system (1) up to twenty days. We can observe tumor cell growth becoming more and more invasive. The optimization parameters are: $\varrho = 0.5 \cdot 10^{-2}$; $\varrho_1 = 10^3$; $\varrho_2 = 2 \cdot 10^4$; $\varrho_3 = 10^6$. The Fig. 3 shows that all constraints are satisfied, and the optimal density of tumor cells ϑ_* decreases, which confirms our expectations. The Fig. 4 presents the optimal control ϕ_* at several days and the Fig. 5 presents the optimal state ϑ_* .

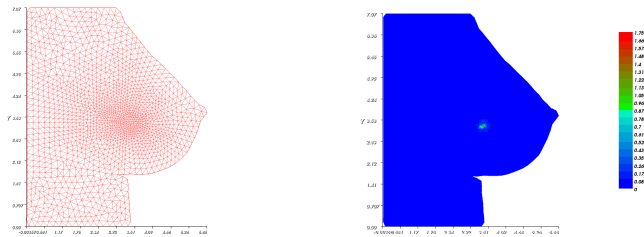


Fig. 1. The breast domain Ω and initial density of tumor cells ϑ_0 .

Remark 3. We have used different scales in Figures 2, 4, and 5 for better visibility of the results. Fig. 6 presents the evolution of the maximum value of optimal control ϕ_* and state ϑ_* in the logarithm scale. This simulation proves that tumor density is drastically reduced.

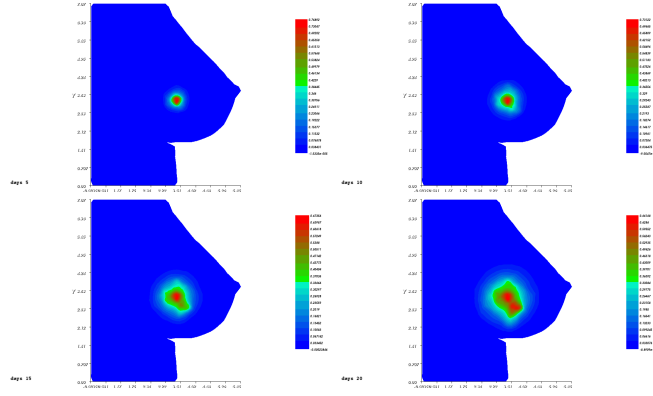


Fig. 2. The density of tumor cells ϑ without treatment at 5^{th} , 10^{th} , 15^{th} , 20^{th} days.

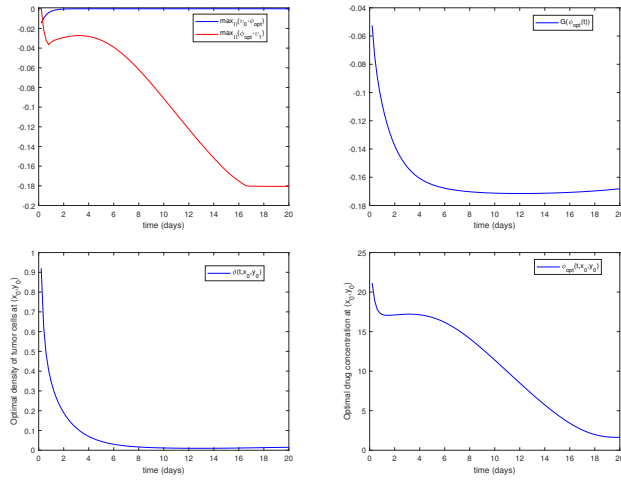


Fig. 3. Constraints satisfaction and the time-evolution of optimal control and state at tumor center.

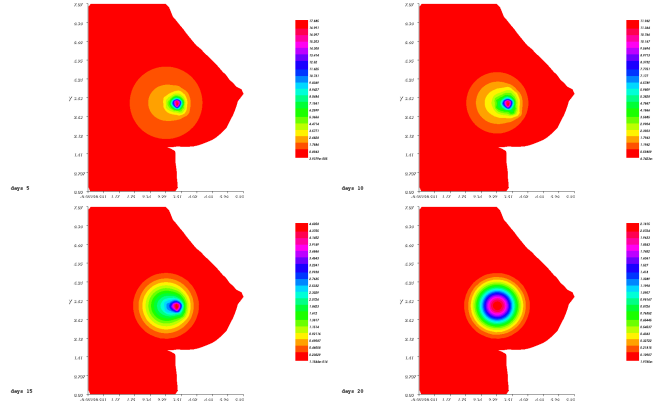


Fig. 4. The optimal drug concentration ϕ_* at 5th, 10th, 15th, 20th days.

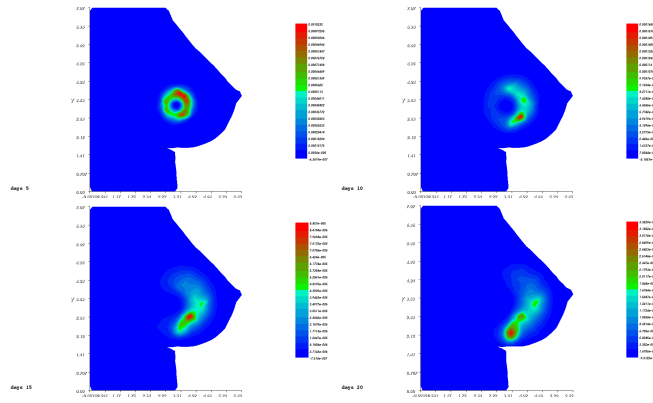


Fig. 5. The optimal density of tumor cells ϑ_* at 5th, 10th, 15th, 20th days.

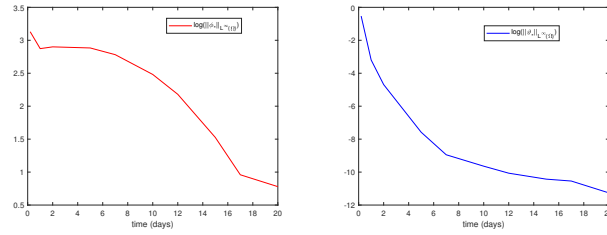


Fig. 6. Evolution of the maximum value of optimal control ϕ^* and state ϑ^* in the logarithm scale.

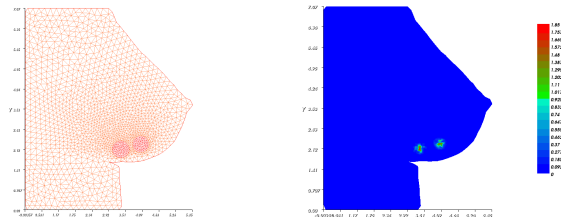
(ii) Case of the presence of two tumors.

In this case, we consider $\vartheta_0(\mathbf{x}) = \eta_1 e^{-\frac{1}{\varepsilon}[(x-x_0)^2+(y-y_0)^2]} + \eta_1 e^{-\frac{1}{\varepsilon}[(x-\tilde{x}_0)^2+(y-\tilde{y}_0)^2]}$, representing the tumor cell density centered at (x_0, y_0) and $(\tilde{x}_0, \tilde{y}_0)$, see Fig. 7. The discretization and mesh information are contained in Table 3.

Table 3. Discretization informations

Parameters	Value	Definitions
Δt	0.2 days (d)	Time Step
\mathbf{x}	$(x; y)$	2D space position
Δx	1 mm	Space Discretizations (x)
Δy	1 mm	Space Discretizations (y)
n_e	3310	Total Mesh Elements
n_p	1716	Total Mesh Points
$(x_0; y_0)$	(10/3; 2.12)	First Tumor center
$(\tilde{x}_0; \tilde{y}_0)$	(4.03; 2.3)	Second Tumor center
$(x_1; y_1)$	(3.68; 2.3)	
ε	0.02	

The Fig. 8 presents the evolution of tumor density cells without treatment. We can observe that the growth of tumor cells is invasive with migration from the breast to other organs. The optimization parameters are as follows: $\varrho = 10^{-2}$; $\varrho_1 = 2 \cdot 10^3$; $\varrho_2 = 10^4$; $\varrho_3 = 3 \cdot 10^6$. The Fig. 9 proves that all constraints are satisfied, and the optimal density of tumor cells ϑ_* decreases to 0. The optimal control ϕ_* and optimal state ϑ_* at several days are given respectively the Fig. 10 and Fig. 11. The Fig. 12 presents evolution in time of the maximum value of optimal control ϕ_* and state ϑ_* .

**Fig. 7.** The breast domain Ω and initial density of tumor cells ϑ_0 .

Remark 4. Once again, we have used different scales in Figures 8, 10, and 11 for better visibility of the results. Even in this case, the simulation proves that tumor density is drastically reduced, and Fig. 12 presents the evolution of the maximum value of optimal control ϕ_* and state ϑ_* in the logarithm scale.

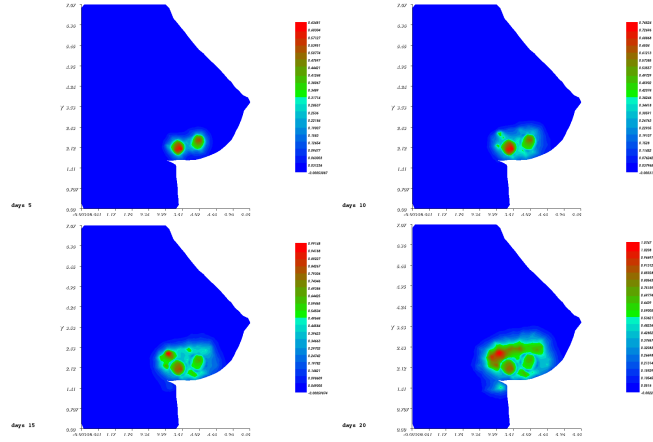


Fig. 8. The density of tumor cells ϑ without treatment at 5th, 10th, 15th, 20th days.

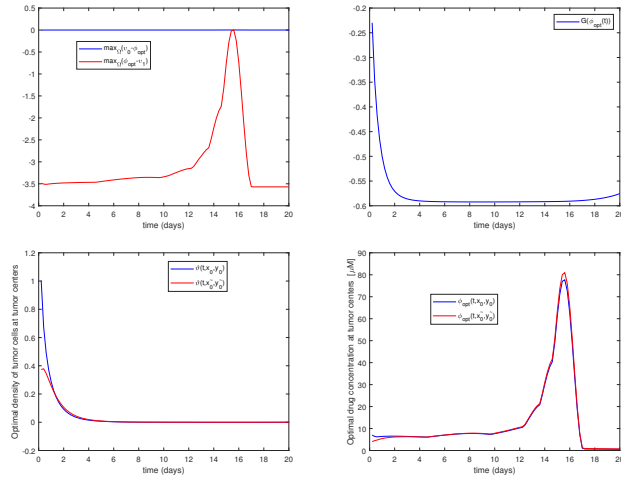


Fig. 9. Constraints satisfaction and the time-evolution of optimal control and state at tumor centers.

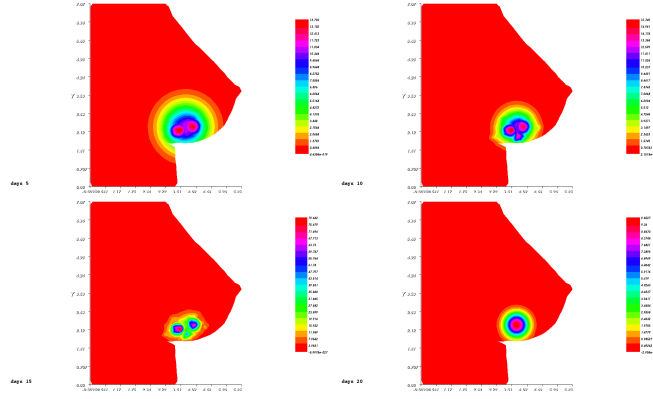


Fig. 10. The optimal drug concentration ϕ_* at 5th, 10th, 15th, 20th days.

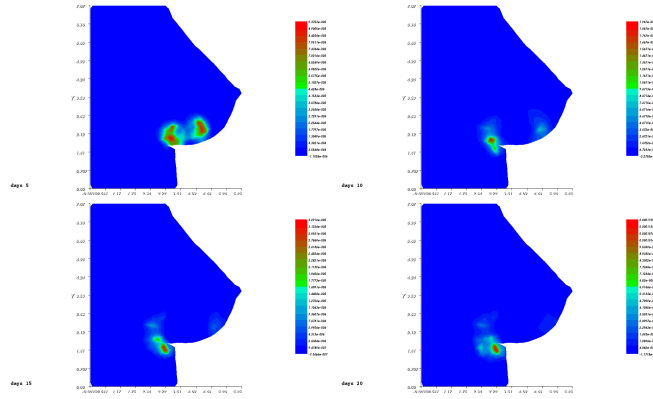


Fig. 11. The optimal density of tumor cells ϑ_* at 5th, 10th, 15th, 20th days.

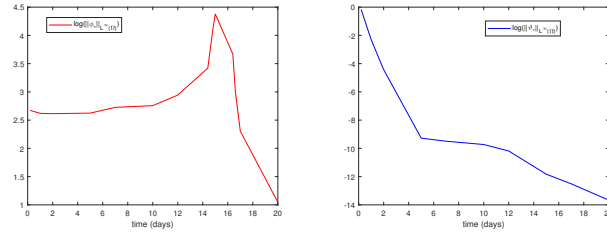


Fig. 12. Evolution of the maximum value of optimal control ϕ_* and state ϑ_* in the logarithm scale.

6 Conclusion and perspectives

In this paper, we present numerical simulations for eradicating malignant breast tumors using the formalism of optimal control problem with state constraint. We show through the simulation results the importance of including constraints on the density of cancer cells. Our numerical approach is based on a mathematical analysis that we proposed in [4]. Due to the continuous temporal and spatial approach (metronomic chemotherapy, see [5] for instance), we developed in this study, we are still far from realistic treatment strategies for malignant breast cancers. In future work, we will develop an approach that is discontinuous in time (chemotherapy cycles) and localized in space (we only act at certain points). Furthermore, it can be interesting to address practical situations with noisy and uncertain data.

Disclosure of Interests. The authors have no competing interests to declare that are relevant to the content of this article.

References

1. Yankeelov, T., Atuegwu, N., Hormuth, D., et al.: Clinically relevant modeling of tumor growth and treatment response. *Science translational medicine* **5**(187), 187ps9, (2013)
2. Lorenzo, G., Hormuth, D., Jarrett A., et al.: Quantitative in vivo imaging to enable tumor forecasting and treatment optimization. e-Preprint arXiv abs/2102.12602, (2021) <https://api.semanticscholar.org/CorpusID:232046193>
3. Belmiloudi, A.: Mathematical modeling and optimal control problems in brain tumor-targeted drug delivery strategies. *International Journal of Biomathematics* **10**(04), 62 p (2017)
4. Lassounon, D., Belmiloudi, A., Haddou, M.: Optimal control problem with mixed control and state constraints for cancer chemotherapy and treatment optimization.
5. Pasquier, E., Kavallaris, M., André, N.: Metronomic chemotherapy: new rationale for new directions. *Nat Rev Clin Oncol* **7**:455-465, (2010)
6. Kimberly M., Rebecca S., Chun L. et al.: Cancer treatment and survivorship statistics, 2016. CA. *Cancer J. Clin.*, **66**(4):271-289, (2016)
7. Swan, G.W.: Role of optimal control theory in cancer chemotherapy. *Math. Biosci.*, **101**(2):237-284, (1990)
8. Swierniak, A., Kimmel, M., Smieja, J.: Mathematical modeling as a tool for planning anticancer therapy. *Eur. J. Pharmacol.*, **625**(1):108-121, (2009)
9. Yin, A., Moes, D., Van Hasselt, J., et al.: A review of mathematical models for tumor dynamics and treatment resistance evolution of solid tumors. *CPT Pharmacometrics Syst. Pharmacol.*, **8**(10):720-737, (2019)
10. Jarrett, A., Hormuth, D., Barnes, S. L., et al.: Incorporating drug delivery into an imaging-driven, mechanics-coupled reaction diffusion model for predicting the response of breast cancer to neoadjuvant chemotherapy: theory and preliminary clinical results. *Phys. Med. Biol.*, **63**(10):105015, (2018)
11. Resende, A., Queiroz, R., Lima, E., et al.: An imaging-driven, mechanical deformation-coupled reaction-diffusion model for describing tumor development. In: XXII ENMC (National Meeting of Computational Modeling) and X ECTM (Meeting of Materials Science and Technology) **5**:1-13, (2020) <https://revistas.ifpr.edu.br/index.php/mundietg/article/view/1040>